Microwave Photonic Photorefractive Smart Filters

Eric Vourc'h, *Student Member, IEEE*, and Didier Hervé

***Abstract*—This paper reviews our past and current work on microwave photonic photorefractive smart filters (MWP-PSFs). These devices rely on the generation of dynamic Bragg gratings inside InP:Fe 1.55-μm photorefractive crystals. First, we concentrate on the applications of MWP–PSFs to optical measurements. We report a 15-pm resolution optical spectrum analyzer without mechanical tuning and a 0.2-nm passive wavelength spaced controller. Secondly, we describe the extension of the MWP-PSF concept to the radio modulation frequency control of fiber-wireless systems. Then, we outline the recent proposal of a wavelength self-tunable single-sideband (WST-SSB) filter in order to compensate for the effects of fiber chromatic dispersion in fiber-radio systems. The performance of the latter device is extensively examined in a fiber-radio 140-Mbit/s data transmission employing binary phase-shift keying modulation at 16 GHz without intermediate frequency. Finally, possible future developments such as the InGaAsP integration of MWP–PSFs and the use of a new photorefractive material are discussed.**

***Index Terms*—Bragg grating, chromatic dispersion, hybrid fiber radio, iron-doped indium phosphide, optical double-sideband signal, optical single-sideband signal, photorefractive effect, radio over fiber, wavelength-division multiplexing.**

I. Introduction

BRAGG gratings are common devices in optical telecommunication areas. They are integrated in lightwave sources such as distributed feedback and distributed Bragg reflector (DBR) laser diodes [1], [2]. They also are used in fiber Bragg grating filters, which are part of the optical add-drop multiplexers implemented in commercial wavelength-division multiplexed (WDM) digital optical-fiber systems [3]. In addition, fiber Bragg gratings can be used as dispersion compensators in long-distance networks [4]. Furthermore, microwave photonic (MWP) signal processing, such as optical beam forming [5] or fiber-optic delay-line filters [6], may also require Bragg gratings. Tunability of the latter devices is often necessary and can be provided by the piezoelectric or magnetostrictive effect [7]. With regards to optically tuned Bragg gratings, these can be achieved at 1.55 μm inside iron-doped indium phosphide (InP:Fe) photorefractive crystals [8]. Indeed, in such a material, an interference pattern due to a 1.55-μm pump beam gives rise to a photorefractive Bragg grating which enables a signal beam whose wavelength is also in the 1.55-μm optical telecommunication range to be diffracted. Of course, since the pump wavelength λ_p controls the period of the Bragg reflector, a tuning of λ_p adjusts the wavelength of the signal to be diffracted λ_s. Additionally, thanks to an InP:Fe response time in the order of a few milliseconds, tuning is relatively fast. Furthermore, the value at which the angle between the beams is set fixes the difference between λ_p and λ_s. Consequently, the wavelength-independent processing of optical signals spaced out by a given wavelength difference is conceivable, so several applications of the latter smart filtering concept have been proposed in the MWP research area [9], [10].

In this paper, we review our past and present work in the field of MWP photorefractive smart filters (PSFs). First, in Section II, we describe the principle of InP:Fe dynamic Bragg gratings. Second, Section III reports applications dedicated to optical instrumentation, that is, a 15-pm resolution spectrum analyzer without mechanical tuning [11] and a passive wavelength spaced controller. Section IV then focuses on fiber-wireless systems applications, that is, the radio modulation frequency control [9] and the compensation for deleterious chromatic dispersion effects by means of a wavelength self-tunable single-sideband (WST-SSB) filter [10]. We report a fiber-radio system experiment at 16 GHz incorporating a WST-SSB filter. A 10^{-9} bit error rate (BER) is achieved after the transmission of a 140-Mbit/s pseudorandom sequence over a 14-km fiber link followed by a 1-m radio link. Finally, in Section V, we consider the InGaAsP/InP:Fe integration prospects of MWP–PSFs [12] and discuss possibilities for reducing the insertion loss of these devices.

II. InP:Fe Microwave Photonic Smart Filter Concept

Photorefractive materials combine light absorption and an electrooptic effect, which allows Bragg gratings to be optically generated. Some photorefractive crystals such as lithium niobate exhibit poor photorefractive effect in the infrared and gratings have to be generated at shorter wavelengths. Filtering can then be obtained in the 1.55-μm wavelength range via a suitable diffraction arrangement. In the case of iron-doped indium phosphide (InP:Fe) and of cadmium telluride (CdTe), both the pump and the probe wavelengths belong to the 1.55-μm optical telecommunication range. The latter property is necessary in order to obtain photorefractive smart filtering. Note that the bandgap of InP is wider than the energy of the 1.55-μm light; however, the presence of the iron traps inside InP:Fe enables the light to be absorbed at that wavelength. From our point of view, InP:Fe is more suitable than CdTe for photorefractive smart filtering. First, InP:Fe response time is fairly short (in the order of a few milliseconds) compared with CdTe response time (in the order of a few seconds). Second, InP:Fe, which is now a

Manuscript received April 16, 2003; revised July 15, 2003.

E. Vourc'h was with the Institut National Polytechnique de Grenoble, Laboratoire de Conception et d'Intégration des Systèmes, Valence Cedex 9, France. He is now with the Laboratory of Systems and Applications of Information and Energy Technologies (SATIE UMR CNRS 8029), Ecole Normale Supérieure de Cachan, 94235 Cachan, France (e-mail: vourch@satie.ens-cachan.fr).

D. Hervé is with the Laboratory of Electronics and Telecommunication Systems (LEST UMR-CNRS 6165), Ecole Nationale Supérieure des Télécommunications de Bretagne, GET–ENST Bretagne, Technopôle de Brest Iroise, 29238 Brest Cedex, France (e-mail: Didier.herve@enst-bretagne.fr).

Digital Object Identifier 10.1109/JLT.2003.821726

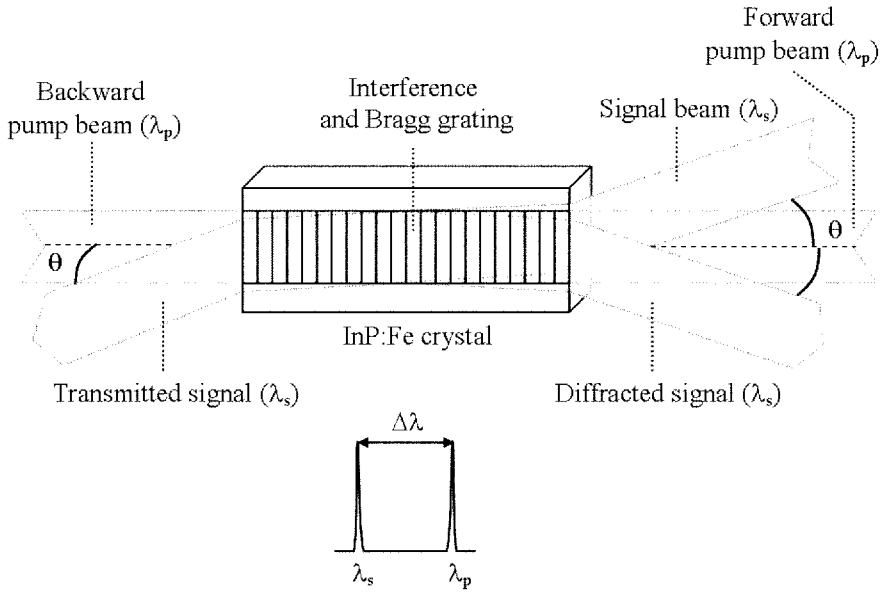

Fig. 1. InP:Fe dynamic Bragg filter scheme.

mass-produced semi-insulating substrate commonly used in optoelctronic devices, is a much more mature material than CdTe. Finally, with regards to integrated optics, InP:Fe/InGaAsP:Fe photorefractive guiding structures are feasible [12].

In order to generate a Bragg grating, an optical interference pattern is generated inside an InP:Fe crystal where light is absorbed and generates free carriers in regions of high intensity. These carriers diffuse and get trapped giving rise to a periodic charge distribution. Given the InP:Fe electrooptic property, the thus obtained periodic space charge field generates periodic refractive index variations. The period Λ of the latter Bragg grating is determined by the illumination configuration responsible for the interference. In the particular case of counterpropagating illumination due to an incident-free spaced pump beam and its reflection off a mirror placed behind the InP:Fe crystal, Λ satisfies (1)

$$\Lambda = \frac{\lambda_{\mathrm{p}}}{2\mathrm{n_m}} \tag{1}$$

where λ_{p} is the pump beam wavelength and $\mathrm{n_m}$ is the InP:Fe average refractive index, which equals 3.17.

A signal beam injected into the crystal at an incident angle θ is reflected by the grating if it satisfies the Bragg diffraction condition (Fig. 1). Equation (2), which assumes counterpropagating illumination, gives the expression for the diffracted signal wavelength λ_{s} according to Snell's law and to the Bragg condition [8]

$$\lambda_{\mathrm{s}} = \lambda_{\mathrm{p}}\sqrt{1-\left(\frac{\sin\theta}{\mathrm{n_m}}\right)^2}. \tag{2}$$

It is to be noted that λ_{s} is lower than λ_{p} and that it belongs to the 1.55-μm telecommunication range as well. In addition, a pump wavelength change simultaneously shifts the period of the grating and the diffracted signal wavelength. Therefore, assuming a fixed, small injection angle, the latter dynamic filter, which is tuned by the pump beam, is associated with an almost fixed wavelength difference $\Delta\lambda = \lambda_{\mathrm{p}} - \lambda_{\mathrm{s}}$(3) for a varying pump wavelength, as well as with an almost-fixed frequency difference Δf(4)

$$\Delta\lambda = \lambda_{\mathrm{p}}\left(1-\sqrt{1-\left(\frac{\sin\theta}{\mathrm{n_m}}\right)^2}\right) \cong \frac{\lambda_{\mathrm{p}}\sin^2\theta}{2\mathrm{n_m^2}} \tag{3}$$

$$\Delta\mathrm{f} = \frac{\mathrm{c}\Delta\lambda}{\lambda_{\mathrm{p}}^2} \cong \frac{\mathrm{c}\sin^2\theta}{2\mathrm{n_m^2}\lambda_{\mathrm{p}}} \tag{4}$$

where c is the speed of light in a vacuum. Indeed, variations of $\Delta\lambda$ and Δf with the pump wavelength in the 40-nm (5000 GHz) band centered on 1550 nm are of 0.005 nm and 0.65 GHz, respectively (Table I). Consequently, the filter enables quasi-wavelength-independent processing of optical signals spaced out by $\Delta\lambda$, that is, spaced out by the associated frequency difference Δf. This yields the capability of smart filtering of microwave photonic signals. The full-width at half-maximum (FWHM) of such a microwave photonic photorefractive smart filter (MWP-PSF) is proportional to the inverse of the grating length L and is independent of θ(5)

$$\mathrm{FWHM} \cong \frac{\mathrm{c}}{2\mathrm{n_m}L}\ (\mathrm{Hz}). \tag{5}$$

Thus, for crystal lengths between 3 and 30 mm, FWHMs lie between 15.8 and 1.6 GHz, respectively. In practice, all the MWP-PSFs used in the applications reported below consist of a 30-mm-long InP:Fe bulk crystal, whose input facet is antireflection coated, a mirror, and three fiber collimators (Fig. 2). Note that, with this configuration, apodization of the filter response is directly obtained [13]. All of the filter elements are glued onto an invar mount whose dilatation coefficient, which is lower than $10^{-6}/^{\circ}$C, avoids θ variations due to temperature variations.

With regards to the crystal orientation, the pump illumination is performed along the $\langle 001\rangle$ axis and, according to the InP:Fe anisotropic properties, this leads to maximum refractive index variations in either the $\langle 110\rangle$ or the $\langle \bar{1}10\rangle$ directions but with opposite signs. This causes polarization sensitivity due

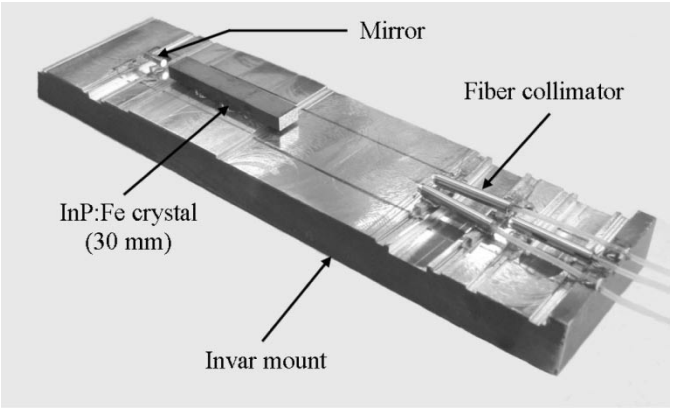

Fig. 2. MWP-PSF setup.

TABLE I
MWP-PSF OPERATING WAVELENGTHS AND FREQUENCIES ($\theta = 2.92°$)

λ_p (nm)	1530.000	1550.000	1570.000
λ_s (nm)	1529.802	1549.800	1569.797
$\Delta\lambda$ (nm)	0.198	0.200	0.203
Δf (GHz)	25.32	24.99	24.67

to coupling variations of the residual two-wave mixing phenomenon for both the pump and the probe beams. The relatively low absorption in InP:Fe at 1.55 μm ($\sim$0.6 dB/cm) is sufficient for the photorefractive effect to take place without giving high propagation losses in the crystal; this leads to a satisfactory trade-off. The electrooptic coefficient of the material being as low as 1.7 pm$\cdot$V^{-1}, refractive index variations are limited. Hence, long crystals are desirable in order to obtain significant diffraction efficiency. In the basic configuration of an MWP-PSF, that is, when the input beams are made up of a single spectral component, the fiber-to-fiber insertion loss of the device is in the order of 17 dB. This value includes the 4.5-dB loss of fiber collimators and the 12.5-dB loss due to low throughput photorefractive effect. It is to be noted that the modulation depth of a grating equals the ratio of the power level of its pump frequency by the total optical power lightening the crystal. As the number of input frequencies increases, the refractive index modulation depth decreases and so does efficiency [13]. The application of an external high voltage electric field onto an MWP-PSF is of no use since carrier diffusion is sufficient and no drift is required in the case of such a very small grating period. Even though many works focus on the performance of photorefractive materials, here we concentrate on demonstrating the feasibility of applications lying mainly in the microwave photonics field. Therefore, we use InP:Fe, which is a mature photorefractive material.

III. MWP-PSF INSTUMENTATION APPLICATIONS

A. Optical Spectrum Analyzer

An optical spectrum analyzer (OSA) without mechanical tuning (Fig. 3) was built based on the association of a tunable three electrode DBR laser, an MWP-PSF, and a computer [11]. The filter, whose characteristics are given in Section II, operates at 37.5 GHz Δf (0.3 nm), and the tuning range of the laser is 1547–1560 nm. The computer, which drives both the Bragg and phase currents of the laser, controls the pump wavelength of the MWP-PSF. Thus, via the Bragg condition, the computer controls the λ_s Bragg wavelength of the filter. In this way, while the optical signal to be analyzed feeds the signal input of the filter, the computer recursively scans λ_s. Since the characteristics of the laser are stored in the memory of the computer, the latter can determine and display the analyzed spectrum thanks to detection of the diffracted signal. In addition, a fixed reference Bragg grating, whose temperature shift is taken into account via a thermal probe, enables measurements to be more accurate. Furthermore, the resolution of the thus obtained OSA equals the FWHM of the filter, which is 15 pm. Although commercial OSAs now usually allow a resolution of the same order, the use of longer crystals could enhance resolution, which makes it of interest for the spectrum analysis of microwave photonic signals as well. With regards to the analysis span, the latter could easily be enhanced by using a four-section DBR laser, which can provide more than 100-nm tuning range [14].

B. Passive Wavelength Spaced Controller

An MWP-PSF can also be used for easy control of the difference between two wavelengths without the need for sophisticated devices. For example, during fabrication, a filter can be set at the given channel spacing of a WDM multiplex. Thus, to control their wavelength spacing, two successive channels of the multiplex can be injected into the signal input and into the pump input of the MWP-PSF, respectively. The power of the diffracted signal is thus a function of the wavelength difference $\Delta\lambda$ and its maximum value corresponds to the desired wavelength spacing. The optical power at both inputs of the filter can be as low as -10 dBm to ensure the generation of the Bragg grating and a measurable reflected signal. Therefore measurement can be performed by removing only a small part of the optical power by means of optical couplers (Fig. 4). The temperature dependence of the refractive index is less than $1.5 \times 10^{-4}/°$C [15], which gives a maximum variation of 0.1 pm/°C when $\Delta\lambda$ is lower than 1 nm. Thus, despite the decrease of the photorefractive coupling coefficient with an increase of the temperature, the device does not require any thermal stabilization. Tunable DBR lasers were tested with these filters and the two wavelengths were simultaneously measured by a 10-pm readout resolution spectrum analyzer in order to verify the validity of the spacing control principle. This kind of device could also be used with a feedback loop when a laser diode has to be monitored by a reference laser. According to (2), the reference wavelength can be either greater or lower than the monitored wavelength depending on which one is chosen to be the writing signal of the Bragg grating.

IV. FIBER-WIRELESS SYSTEM APPLICATIONS

A. MWP-PSF Under DSB Illumination

Fiber-wireless systems [16] that associate optical and radio-frequency (RF) techniques are receiving a great deal of attention with a view to future broadband access networks. First, optical

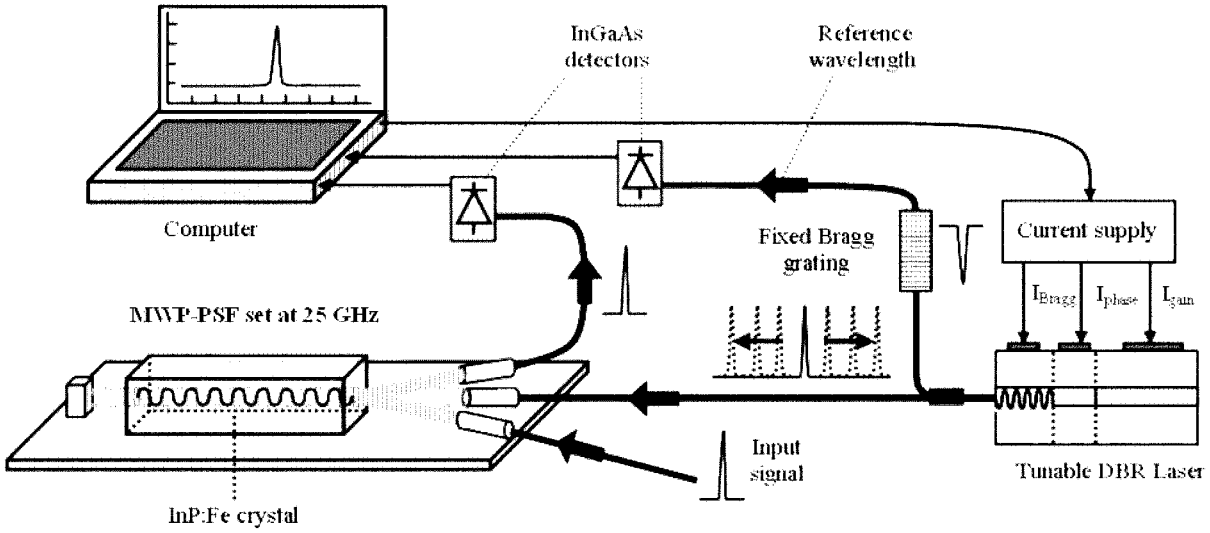

Fig. 3. Optical spectrum analyzer without mechanical tuning implementing a three-section tunable DBR laser, an MWP-PSF set at 25 GHz, and a computer.

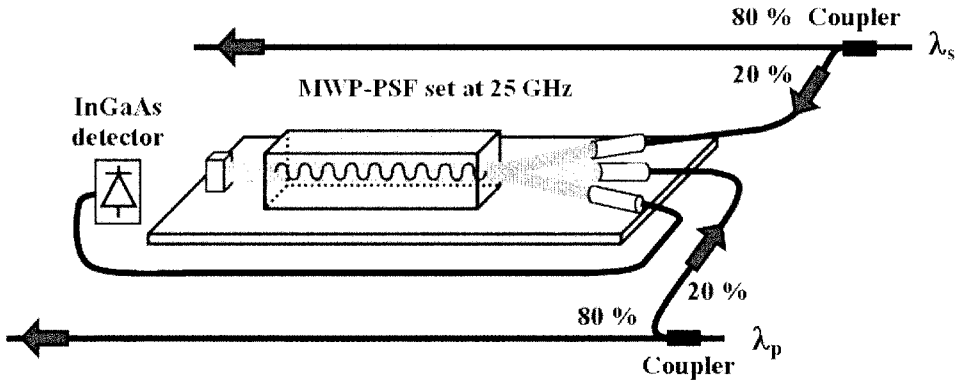

Fig. 4. Experimental setup for wavelength spacing control using an InP:Fe MWP-PSF.

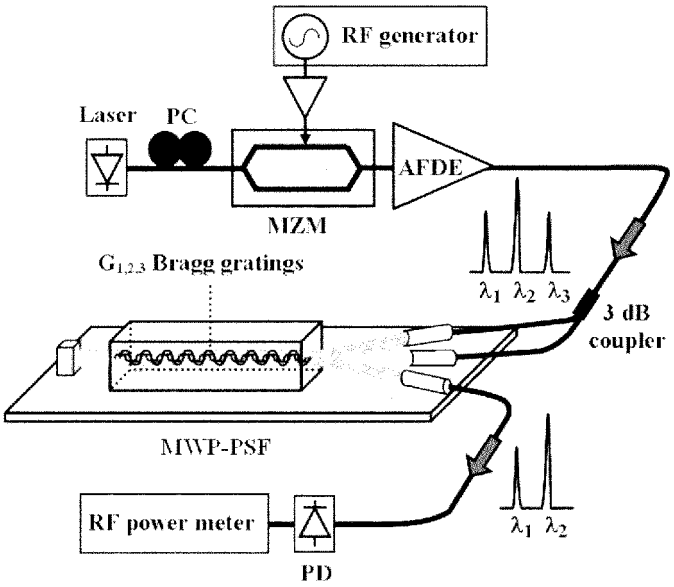

Fig. 5. Characterization experiment of an MWP-PSF under DSB illumination.

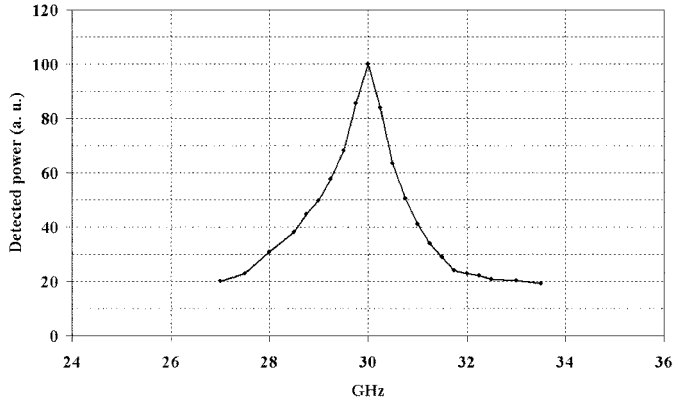

Fig. 6. Detected power at the output of an MWP-PSF set at 30 GHz as a function of the modulation frequency of the input DSB signal (a.u.: arbitrary unit).

fibers enable significant data rates to be transported from a central station up to remote base stations. Second, deployment of radio links over the last miles of the network turns out to be cost-competitive compared with wired access. Standard hybrid fiber-radio systems use RF intensity modulated optical signals, whose spectrum consists of the optical carrier and two sidebands. The $\Delta\lambda$ wavelength difference between the lines of such a double sideband (DSB) signal is a function of the f_m RF (6)

$$f_m = \frac{c\Delta\lambda}{\lambda_c^2} \tag{6}$$

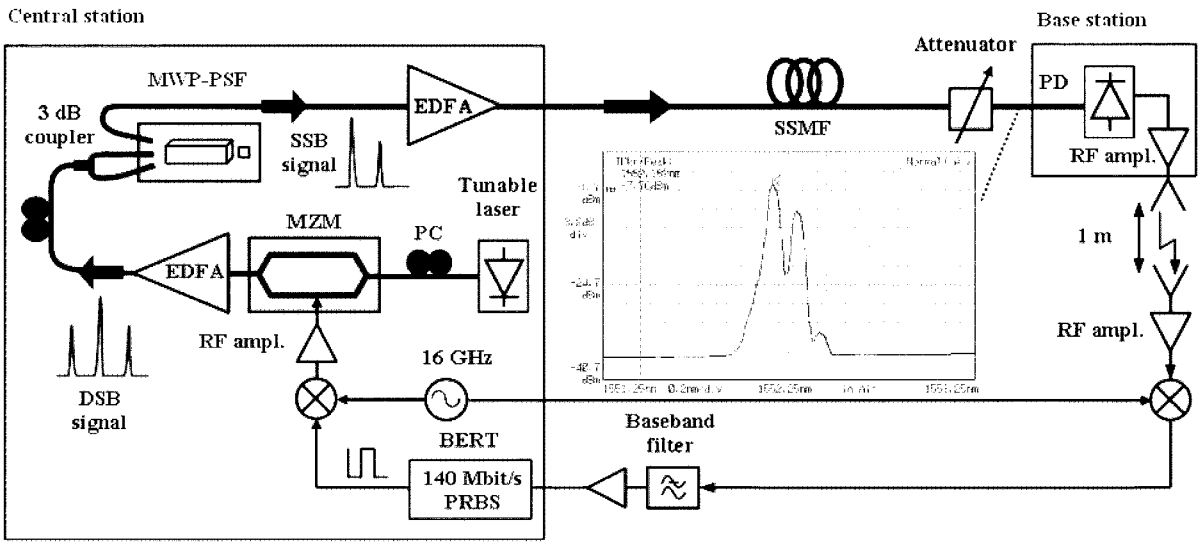

Fig. 7. Experimental setup for the fiber-radio transmission of a BPSK 140-Mbit/s data stream at 16 GHz. The SSB signal containing the data is transported over a 14-km SSMF link followed by a 1-m radio link (BERT: bit error rate testset). Inset shows the SSB signal measured at the base station.

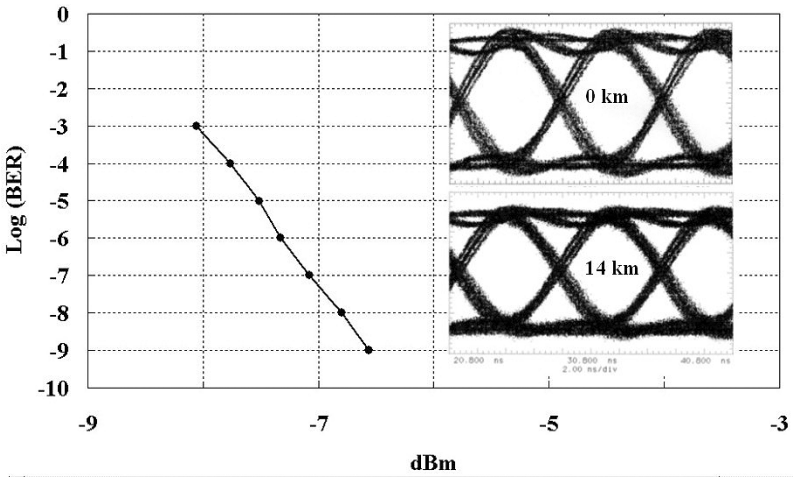

Fig. 8. Detected BER as a function of the received optical power after a 14-km SSMF link followed by a 1-m radio link. Inset shows the measured eye pattern of the received data corresponding to 0- and 14-km fiber links.

where λ_c is the optical carrier wavelength.

The similarity between (4) and (6) led us to study and investigate the injection of a DSB signal into an MWP-PSF, whose Δf operating frequency was set to f_m. In such a configuration (Fig. 5), each interference pattern due to a $\lambda_i (i = 1,2,3)$ line of the DSB pump beam gives rise to a G_i Bragg grating. In addition, since $\Delta f = f_m$, a λ_i signal beam line and a λ_{i+1} pump beam line satisfy the diffraction condition of the filter (2). Consequently, G_2 and G_3 gratings diffract signal lines λ_1 and λ_2, respectively, while the λ_3 signal line is not diffracted. Such a property could be exploited with the aim of controlling the modulation frequency of an intensity modulated optical signal at either a microwave or a millimeter-wave frequency [9].

Fig. 5 depicts the experimental setup for measuring the output detected frequency of an MWP-PSF under DSB illumination. External modulation of a DBR laser by means of a Mach–Zehnder modulator (MZM) provided a DSB signal that was amplified by an erbium-doped fiber amplifier (EDFA) and then launched into a 3-dB coupler connected to the inputs of an MWP-PSF. The latter filter operated at 30 GHz and the MZM was driven by an RF generator whose frequency could be tuned from 27 to 33.5 GHz. Finally, a photodiode (PD) placed at the filter output enabled us to detect the average value of the diffracted signal as a function of the RF frequency. According to this measurement (Fig. 6), the central operating frequency of the filter used is 30 GHz and the FWHM is in the order of 1.82 GHz, which agrees with predictions (5). It is to be noted that for stability of the diffracted signal, a fiber portion (not depicted) with a greater length than the coherence length of the laser was inserted in the pump path of the coupler. This enabled us to avoid two-wave-mixing and undesirable photorefractive effect due to the signal beam.

B. WST-SSB Filter

Future fiber-wireless access networks will require mitigation of chromatic dispersion effects, especially in architectures implementing radio-over-fiber transport [17]. Techniques, such as

TABLE II
POWER REPORT OF THE FIBER-RADIO TRANSMISSION

Device	Average optical power (dBm)	AC electrical power (dBm)
Laser	3.4	
MZM	-5.7	
EDFA 1	11.3	
MWP-PSF	-20.0	
EDFA 2	6.0	
SSMF (14 km)	1.4	
PD		-27.7
RF amplifier 1		6.3
Transmitter antenna		22.1
Radio link (1 m)		-30.8
Receiver antenna		-15.0
RF amplifier 2		1.3
Mixer		-8.6
Baseband filter		-8.8
BF amplifier		11.2

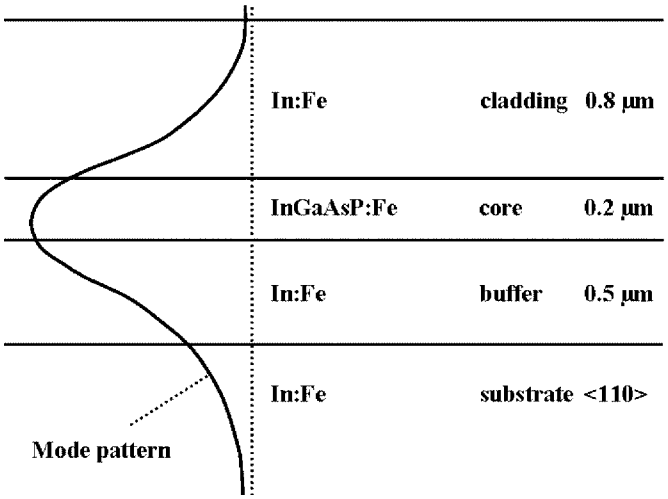

Fig. 9. Planar waveguide structure.

"up-conversion" [18] or the application of a negative chirp onto an MZM [19] could be useful as they alleviate the chromatic dispersion power penalty, which may occur at the base station as a function of the fiber length from the central station [20]. However, in the millimeter-wave domain, the use of optical SSB signals may be preferred as it completely eliminates the fading phenomenon of the photodetected power level experienced when DSB signals are used [19]. Optical SSB signals can be generated thanks to interferometry techniques using either a dual electrode MZM [19] or two electroabsorption modulators [21]. Another possibility lies in the SSB filtering of one sideband of a DSB signal by means of a fixed Bragg grating [22]. Although very simple, the latter technique requires a narrow-band Bragg filter and is dependent on the wavelength of the optical carrier. Alternatively, an MWP-PSF operating at the suitable radio frequency can filter a DSB signal provided that it is in the 1.55-μm wavelength range [10]. Indeed, since a part of the input DSB signal to be filtered generates the Bragg gratings, the filter is wavelength self-tunable (WST).

To demonstrate the latter concept, the radio-over-fiber transport of a 16-GHz binary phase-shift keyed (BPSK) carrier with a 140-Mbit/s data stream was implemented (Fig. 7). The SSB generation scheme involved an MWP-PSF placed at the central station. The operating frequency of the latter WST-SSB filter equaled the RF carrier value, that is, 16 GHz. The thus generated SSB signal containing data was transmitted over a standard single-mode fiber (SSMF) link, whose length was 14 km. Then, the RF signal photodetected at the base station was transmitted over a 1-m radio link before being received and subsequently down-converted. Finally, BERs were measured as a function of the optical power before the PD (Fig. 8). A 10^{-9} BER was achieved for a 1.4-dBm optical power level at the base station. It is to be noted that tuning the optical carrier wavelength did not affect the BER, which demonstrates the wavelength self-tunability of the SSB filtering technique used. In addition, given a constant optical power, the maximum detected RF power degradation observed as a function of the length of the SSMF link was 1 dB [10].

According to the power report of the transmission (Table II), the fiber-to-fiber efficiency of the filter, that is, the difference between the input and output average optical power levels of the MWP-PSF, was -31.3 dB. Therefore, an EDFA was necessary in order to partly compensate the loss. Such amplification was done at the expense of an optical signal-to-noise ratio degradation. Error-free data transmission was achieved even without an amplified spontaneous emission filter. In fiber-radio access networks, WDM techniques can both increase the throughput capacity and simplify signal routing [23]. In addition, the use of arrayed waveguide gratings mutiplexers enables chromatic dispersion effects to be mitigated [24]. In our case, a two-SSB-channel WDM configuration implementing an MWP-PSF has also been demonstrated, showing good transmission performance [25], but, as mentioned in Section II, the diffraction efficiency of the filter decreases as the number of superimposed gratings increases [13]. In the current state of the art, a high loss may make WST-SSB filters difficult to use in practice. However, the following section discusses integration prospects of MWP-PSFs that may improve the device's reflectivity.

Finally, with regard to the technical requirements of a WST-SSB filter used in a real environment, first, the input power level should be in the order of 10–13 dBm and, second, polarization should be controlled. Indeed WST-SSB filters exhibit a polarization sensitivity up to 9 dB; however this is no longer a drawback when WST-SSB filters are transmitter devices. Given the temperature sensitivity of the efficiency of the photorefractive effect inside InP:Fe, control of the temperature would also be useful in a real environment.

V. INTEGRATION PROSPECTS

An integrated MWP-PSF structure was designed and realized instead of the bulk InP:Fe crystal filter previously reported. By confining a given light power in a waveguide structure, the rise in optical intensity increases the index variation if compared with the bulk configuration and also increases the speed of the grating generation [12]. In addition, photorefractive waveguides have the advantage of being compatible with optoelectronic device integration. A slab waveguide was built on a semi-insulating $\langle 110 \rangle$ oriented InP:Fe substrate by

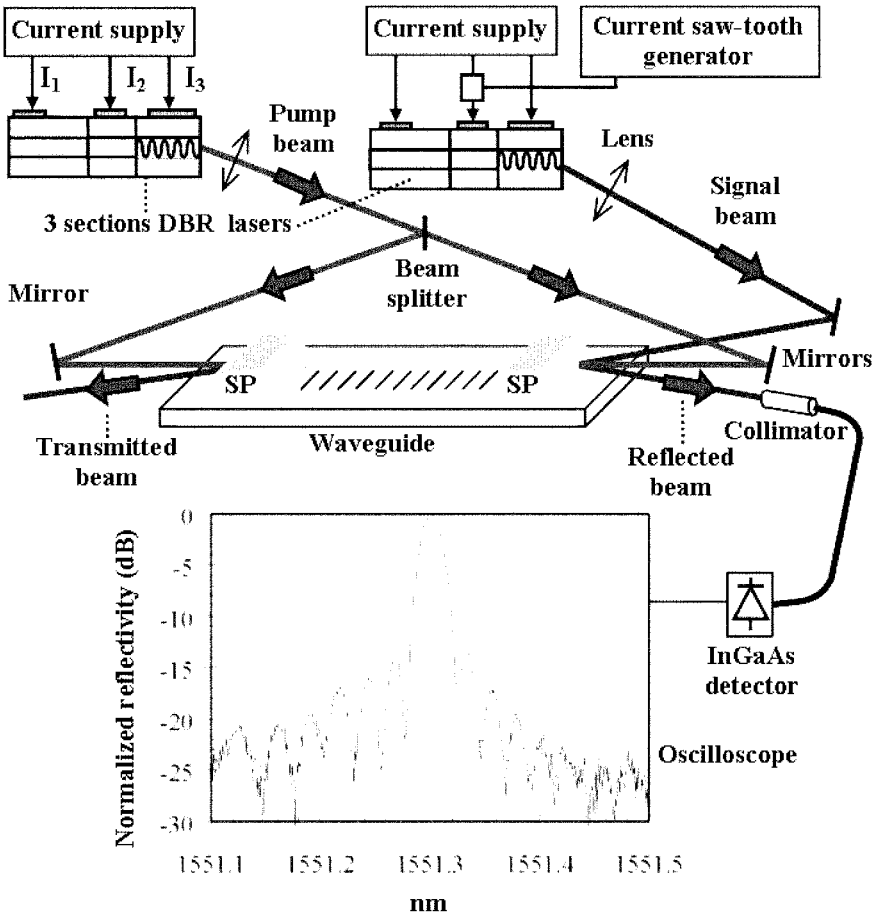

Fig. 10. Experimental setup for the characterization of the InGaAsP:Fe/InP:Fe photorefractive waveguide. Inset shows the measured spectral response of the dynamic Bragg grating generated inside the photorefractive planar waveguide structure.

gas source molecular beam epitaxy. The waveguide core is a GaInAsP:Fe ($\lambda_g = 1.1$ μm) layer of 0.2-μm thickness. The lower buffer and upper cladding are both InP:Fe layers (0.5 and 0.8 μm thick, respectively). The Fe concentration is 10^{17} cm^{-3} in the epitaxial layers, and the concentration of ionized traps is enhanced by Si doping (10^{16} cm^{-3}) [26].

Taking into account the higher absorption in the core layer, the mode pattern is designed so that some 75% of the optical energy propagates in the InP:Fe material (Fig. 9). This mode pattern is also effective for the photorefractive effect in InP:Fe. The thus obtained MWP-PSF in a photorefractive waveguide is not as compact as the previous fibered filter because silicon prisms are used for the input and output coupling for easy testing of the slab waveguide device (Fig. 10). The interaction length L is evaluated as the distance between the prisms, which is chosen to be equal to 18 mm. Tuning the signal wavelength while keeping a fixed pump wavelength enabled us to measure the reflectivity of the filter via the photodetected output signal. The measured spectral response, which is shown in the inset of Fig. 10, is characteristic of a Bragg grating. The measured FWHM is 0.02 nm, which is the same as the value that would be obtained for a bulk crystal filter. The maximum reflectivity has a value of 2% (-17 dB) corresponding to the ratio between the maximum reflected signal and the transmitted signal. The measured response time is 250 μs, which is 20 times lower than that obtained for a bulk MWP-PSF. Despite the low prism coupling, these results show that the optical intensity is much higher in the waveguide than in the bulk crystal. Note that the θ angle was set to 2.4°, which leads to a $\Delta\lambda$ of 0.14 nm. Thus, we have demonstrated the feasibility of a photorefractive Bragg grating inside a waveguide. This is a first step in the design of an integrated MWP-PSF, which could lead to a device with improved reflectivity if compared with bulk ones. A fully integrated filter incorporating separate branching waveguides instead of prism couplers could be considered. Regarding the loss reduction of MWP-PSFs, a device using a CdTe photorefractive bulk crystal could also be envisaged since the electrooptic coefficient of this material (5.5 pm·V^{-1}) is higher than the InP:Fe coefficient (1.7 pm·V^{-1}) [27]. In that case, the expected throughput increase could be several dBs.

VI. Conclusion

In this paper, we have reviewed our past and ongoing work dealing with microwave photonic photorefractive smart filters. We have given an extensive description of the setup and characteristics of such devices, the principle of which lies in the exposure to interference of a photorefractive crystal sensitive to a

1.55-μm optical excitation leading to Bragg grating generation. Given a fixed injection angle, the thus obtained filter enables the diffraction of spectral components corresponding to a fixed frequency difference Δf with respect to the pump spectrum. We have been concerned with reporting a variety of applications lying in the microwave photonics field. The first application that has been built is a 15-pm resolution optical spectrum analyzer without mechanical tuning. In addition, we have reported for the first time a passive wavelength spaced controller dedicated to WDM systems.

With regards to the fiber-radio research area, we have proposed the RF control of such a system by means of an MWP-PSF. We have also outlined our recent work dealing with wavelength self-tunable single-sideband filtering with a view to overcoming chromatic dispersion effects in hybrid fiber-radio systems. We have reported a fiber radio 140-Mbit/s data transmission at 16-GHz RF and have provided a detailed power report of the transmission as well as BER measurements showing a 10^{-9} BER at 1.4-dBm received optical power. Every MWP-PSF implemented in the applications reported here uses an InP:Fe photorefractive crystal. This material has been chosen for its maturity. In addition, InP:Fe has the advantage of a relatively fast response time. On the other hand, InP:Fe has a very low photorefractive effect throughput at 1.55 μm. However, our main purpose was not to reach an overall performance but to concentrate on the originality of the MWP-PSF concept and to demonstrate the feasibility of microwave photonic signal processing. Nevertheless, as finally discussed, the throughput performance of MWP-PSFs could benefit by several dBs from an InGaAsP:Fe/InP:Fe integrated structure. Alternately, another photorefractive material with a higher electrooptic coefficient such as CdTe could also improve the reflectivity. New investigations are being carried out in order to extend the SSB technique to wide-band signals such as 10-Gbit/s streams. Not only are SSB signals of great interest to overcome dispersion but also they have an improved spectral efficiency, which is desirable for DWDM systems.

ACKNOWLEDGMENT

The authors wish to acknowledge the assistance and support of France Telecom R&D Lannion-France. They are particularly grateful to R. Coquillé for providing the InP:Fe crystals. The authors would also like to thank their academic colleagues from ENST Bretagne, Brest, France, M. Gravot, J. Ormrod, D. Bourreau, B. Della, P. McLaughlin, C. Person, and S. Pinel for their many contributions to the work reported in this paper.

REFERENCES

[1] W. Streifer, R. D. Burnham, and D. R. Scifres, "Effect of external reflectors on longitudinal modes of distributed feedback lasers," *IEEE J. Quantum Electron.*, vol. QE-11, pp. 154–161, 1975.

[2] T. L. Koch and U. Koren, "Semiconductor lasers for coherent optical communications," *J. Lightwave Technol.*, vol. 8, pp. 274–293, Mar. 1990.

[3] C. R. Giles, "Lightwave applications of fiber Bragg gratings," *J. Lightwave Technol.*, vol. 15, pp. 1391–1404, Aug. 1997.

[4] F. Ouellette, "Dispersion cancellation using linearly chirped Bragg grating filters in optical waveguides," *Opt. Lett.*, vol. 12, no. 10, pp. 847–849, Oct. 1987.

[5] R. A. Minasian and K. E. Alameh, "Optical-fiber grating based beamforming network for microwave phased arrays," *IEEE Trans. Microwave Theory Tech.*, vol. 45, pp. 1513–1518, Aug. 1997.

[6] J. Capmany, D. Pastor, and B. Ortega, "New and flexible fiber-optic delay lines filters using chirped Bragg gratings and laser arrays," *IEEE Trans. Microwave Theory Tech.*, vol. 47, pp. 1321–1326, July 1999.

[7] X. Z. Lin, Y. Zhang, H. L. An, and H. D. Liu, "Electrically tunable singlemode fiber Bragg reflective filter," *Electron. Lett.*, vol. 30, no. 11, pp. 887–888, 1994.

[8] D. Hervé, M. Chauvet, J. E. Viallet, and M. J. Chawki, "First tunable narrowband 1.55 μm optical drop filter using a dynamic photorefractive grating in iron doped indium phosphide," *Electron. Lett.*, vol. 30, pp. 1883–1884, 1994.

[9] D. Hervé, J. F. Cadiou, R. Coquillé, and S. Pinel, "A novel photonic technique using a dynamic bragg grating in InP:Fe for microwave modulation frequency control of fiber-wireless systems," in *IEEE Int. Topical Meeting Microwave Photonics (MWP'99)*, Melbourne, Australia, Nov. 1999, pp. 227–230.

[10] E. Vourc'h, D. Le Berre et, and D. Hervé, "Lightwave single side-band wavelength self–tunable filter using an InP:Fe crystal for fiber–wireless systems," *IEEE Photon. Technol. Lett.*, vol. 14, pp. 194–196, Feb. 2002.

[11] D. Hervé, M. Chauvet, J. E. Viallet, and M. J. Chawki, "Narrow-band WDM spectrum analyzer without mechanical tuning," *Electron. Lett.*, vol. 32, pp. 838–839, 1996.

[12] D. Hervé, J. E. Viallet, S. Salaün, A. Le Corre, F. Delorme, and B. Mainguet, "Tunable narrowband optical filter in photorefractive InGaAsP:Fe/InP:Fe singlemode waveguide," in *Proc. Int. Conf. Indium Phosphide and Related Materials (IPRM'97)*, Hyannis, MA, 1997, pp. 107–110.

[13] E. Vourc'h and D. Hervé, "Wavelength–Self–Tunable single side-band InP:Fe filter model," in *Proc. IEEE/IEICE Microwave Photonics (MWP'02)*, Nov. 2002, pp. 185–188.

[14] F. Delorme, "Widely tunable 1.55-μm lasers for wavelength-division-multiplexed optical fiber communications," *IEEE J. Quantum Electron.*, vol. 34, pp. 1706–1716, Sept. 1998.

[15] G. D. Pettit and W. J. Turner, "Refractive index of InP," *J. Appl. Phys.*, vol. 36, p. 2081, 1965.

[16] A. J. Seeds, "Broadband fiber-radio access networks," in *Proc. IEEE Microwave Photonics (MWP'98)*, 1998, pp. 1–4.

[17] M. Goloubkoff, E. Penard, D. Tanguy, and P. Legaud, "Outdoor and indoor applications for broadband local loop with fiber supported mm-wave radio systems," in *Proc. IEEE Microwave Theory Tech Symp. (MTT-S'97)*, vol. 1, June 1997, pp. 8–13.

[18] J. M. Fuster, J. Marti, V. Polo, F. Ramos, and J. L. Corral, "Chromatic dispersion effects in electro-optical upconverted millimeter-wave fiber optic links," *Electron. Lett.*, vol. 33, pp. 1969–1970, Nov. 1997.

[19] G. H. Smith, D. Novak, and Z. Ahmed, "Overcoming chromatic-dispersion effects in fiber-wireless systems incorporating external modulators," *IEEE Trans. Microwave Theory Tech.*, vol. 45, pp. 1410–1415, Aug. 1997.

[20] G. J. Meslener, "Chromatic dispersion induced distortion of modulated monochromatic light employing direct detection," *IEEE J. Quantum Electron.*, vol. QE-20, pp. 1208–1216, 1984.

[21] E. Vergnol, F. Devaux, D. Tanguy, and E. Pénard, "Integrated lightwave millimetric single side-band source: Design and issues," *J. Lightwave Technol.*, vol. 16, pp. 1276–1284, July 1998.

[22] Park, W. V. Sorin, and K. Y. Lau, "Elimination of the fiber chromatic dispersion penalty on 1550 nm millimeter-wave optical transmission," *Electron. Lett.*, vol. 33, pp. 512–513, Mar. 1997.

[23] A. Nirmalathas, C. Lim, D. Novak, D. Castleford, R. Waterhouse, and G. Smith, "Millimeter-wave fiber-wireless access systems incorporating wavelength division multiplexing," in *Microwave Conf.*, Asia Pacific, 2000, pp. 625–629.

[24] J. Capmany, D. Pastor, P. Munoz, B. Ortega, S. Sales, and A. Martinez, "Multiwavelength optical SSB generation for dispersion mitigation in WDM fiber radio systems using AWG multiplexer," *Electron. Lett.*, vol. 38, no. 20, pp. 1194–1196, Sept. 2002.

[25] E. Vourc'h, D. Le Berre, and D. Hervé, "Millimeter-wave power fading compensation for WDM fiber-radio transmission using a wavelength-self-tunable single sideband filter," *IEEE Trans. Microwave Theory Tech.*, vol. 50, pp. 3009–3015, Dec. 2002.

[26] M. Chauvet, D. Hervé, B. Mainguet, R. Rébéjac, S. Salaün, A. Le Corre, and J. E. Viallet, "Photorefractive semiconductor single-mode waveguide grown by gas-source molecular-beam epitaxy," *Opt. Lett.*, vol. 20, no. 15, pp. 1604–1606, 1995.

[27] P. Yeh, "Introduction to photorefractive nonlinear optics," in *Wiley Series in Pure and Applied Optics*, J. W. Goodman, Ed. New York: Wiley, 1993, pp. 26–27.

Eric Vourc'h (S'03) was born in Brest, France, in 1974. He received the B.S. degree in physics and the M.S. and Ph.D. degrees in electrical and electronic engineering from the University of Brest, Brest, France, in 1998, 1999, and 2002, respectively.

From 1999 to 2002, he has been with the Laboratory of Electronics and Telecommunication Systems (LEST), which is run jointly by the Ecole Nationale Supérieure des Télécommunications de Bretagne (ENST-Bretagne/French National School of Telecommunications Engineering of Brittany) and the University of Brest. From October 2002 to August 2003, he was an Assistant Lecturer at the Institut National Polytechnique de Grenoble, Valence, France. In September 2003, he joined the Ecole Normale Supérieure de Cachan (ENS Cachan), Cachan, France, where he is currently an Associate Professor. His research interests include optical signal processing, fiber-wireless communication systems, and optical communication systems.

Mr. Vourc'h received First Prize in the student paper competition of the 2001 IEEE International Topical Meeting on Microwave Photonics (January 2002) and the Best Poster Paper Award of the 2002 IEICE/IEEE International Topical Meeting on Microwave Photonics (November 2002). He also received the International Engineering Consortium's William L. Evritt Student Award of Excellence (May 2002).

Didier Hervé was born in Treguier, France, in 1962. He received the B.S. degree in electrical and electronic engineering and the M.S. and Ph.D. degrees from the University of Brest, Brest, France, in 1984, 1992, and 1996, respectively.

He worked at France Telecom as a Switching Exchange Technical Manager in Paris, France, from 1985 to 1988. In 1989, he joined the teaching Staff of the Microwave Department, Ecole Nationale Supérieure des Telecommunications de Bretagne in Brest (ENST Bretagne/French National School of Telecommunications Engineering of Brittany). His doctoral studies involved research on dynamic Bragg gratings in iron doped indium phosphide and photorefractive waveguide structures in III–V compounds. This work was carried out jointly with France Telecom Research & Development Center in Lannion. From October 1997 to April 1998, he was a Visiting Scholar at the University of Sydney, Australia, where he worked on a project including fiber Bragg gratings for optical signal-processing applications. His current research activities are focused on the microwave photonics field and particularly on hybrid fiber-wireless distribution systems. Since he became an Associate Professor in 1998 he has also been working with the international relations division at ENST Bretagne for student exchange programs, mainly with Australia and Spain. Since 2002, he is involved in the Fiber-Radio Group, ITACA Research Institute, Universidad Politécnica de Valencia, Valencia, Spain.